Research Square

Preprints are preliminary reports that have not undergone peer review.
They should not be considered conclusive, used to inform clinical practice,
or referenced by the media as validated information.

Unveiling the Phase Structure of a Spin-$1/2$ XXZ Chain with Four-Spin Cluster Interactions through Quantum Correlations

Mohammad Ababsi
University of Guilan
Saeed mahdavifar
smahdavifar@gmail.com
University of Guilan
George Japaridze
Ilia State University

Article

Keywords:

Posted Date: November 23rd, 2026

DOI: https://doi.org/10.21203/rs.3.rs-11667201/v1

License: This work is licensed under a Creative Commons Attribution 4.0 International License.
Read Full License

Additional Declarations: No competing interests reported.

Unveiling the Phase Structure of a Spin-$1/2$ XXZ Chain with Four-Spin Cluster Interactions through Quantum Correlations

M. Abbasi[1], **S. Mahdavifar**[*1], **and G. I. Japaridze**[2,3]

[1]Department of Physics, University of Guilan, 41335-1914, Rasht, Iran
[*]smahdavifar@gmail.com
[2]Ilia State University, Chavchvadze Avenue 43, 0162 Tbilisi, Georgia
[3]Andronikashvili Institute of Physics, Tamarashvili str. 6, 0177 Tbilisi, Georgia

ABSTRACT

We investigate the ground-state phase structure and quantum correlations of a one-dimensional spin-$1/2$ XXZ chain with four-spin cluster interactions. Combining exact diagonalization, density-matrix renormalization group calculations, and an analytical mean-field approach, we characterize the evolution of the ground state as a function of the anisotropy parameter. For finite cluster coupling, we identify three distinct regimes, consisting of a ferromagnetic phase, an intermediate gapless phase, and a N'eel phase. The first transition from the ferromagnetic to the gapless phase is clearly manifested in the ground-state energy, its derivatives, the longitudinal spin correlations, and the magnetization. In contrast, the second transition toward the N'eel phase leaves only a weak signature in conventional finite-size quantities, making its precise determination difficult from the ground-state energy and the staggered spin structure factor alone. To overcome this limitation, we investigate quantum correlations through the nearest-neighbor concurrence and quantum discord. The concurrence exhibits a pronounced maximum at the second critical point, while the quantum discord provides distinct signatures of both phase transitions, including a cusp at the second critical point. Our results demonstrate that quantum-information measures can provide sensitive probes of phase boundaries that are difficult to resolve using conventional finite-size observables, and offer a useful framework for characterizing quantum phase transitions in spin chains with multispin interactions.

1 Introduction

In quantum many-body systems, interactions extending beyond conventional pairwise exchange can give rise to collective phenomena that are qualitatively different from those encountered in systems governed solely by two-spin couplings. In particular, multispin and cluster interactions provide an important route for generating nontrivial many-body correlations, unconventional quantum phases, and characteristic low-energy excitations in quantum spin systems. Such interactions naturally arise in effective spin Hamiltonians when the underlying microscopic degrees of freedom are integrated out, and can also emerge from higher-order exchange processes involving several magnetic sites. Their presence has been identified in a variety of magnetic systems, where higher-order and anisotropic interactions can complement the dominant Heisenberg exchange and substantially influence the resulting magnetic properties[1–3]. Beyond their relevance to quantum magnetism, controlled many-body interactions are also of considerable interest for quantum technologies, where they provide resources for engineering and manipulating highly correlated quantum states, quantum simulation, and quantum information processing[4,5]. These features make spin chains with multispin interactions particularly useful theoretical platforms for exploring how competing many-body interactions shape quantum phases and quantum critical phenomena.

In addition to theoretical interest, four-spin and other multispin exchange interactions are relevant to a range of correlated materials, where higher-order exchange processes can modify magnetic excitations and low-energy spectral properties. Evidence for such interactions has been reported in quasi-one-dimensional cuprates and copper-oxide ladder compounds, including La_2CuO_4, $La_6Ca_{28}Cu_{24}O_{41}$, and $La_4Sr_{10}Cu_{24}O_{41}$[6–9]. Related multispin exchange mechanisms have also been discussed in hydrogen-bonded ferroelectrics and squaric acid crystals[10–13]. Beyond naturally occurring materials, optical-lattice platforms offer opportunities to engineer effective multispin interactions in controlled geometries, providing a route to investigate their effects on quantum correlations and ground-state properties[14,15]. These realizations underscore the physical relevance of interactions beyond pairwise exchange and motivate investigations of how multispin couplings influence quantum phases, critical behavior, and the low-energy properties of quantum magnets.

The classification of quantum phases of matter is a central problem in condensed-matter physics[16]. Within the conventional

Landau paradigm, distinct phases are identified through local order parameters associated with spontaneous symmetry breaking, while quantum phase transitions correspond to qualitative changes in the ground-state structure induced by quantum fluctuations[17]. This framework has provided a powerful description of a broad range of quantum many-body systems, including quantum spin chains and magnetic systems. However, it does not provide a complete characterization of all possible quantum phases[18,19]. In particular, quantum phases may lack a conventional local order parameter while remaining sharply distinct because of their global quantum structure. This limitation has motivated the development of complementary approaches based on topology, quantum entanglement, and symmetry properties.

Among one-dimensional quantum spin systems, the spin-$1/2$ XY model occupies a central position as a paradigmatic model for studying quantum fluctuations, quantum criticality, and collective excitations in interacting spin chains. Its exchange interaction,

$$H_{XY} = J\sum_{n}\left(S_n^x S_{n+1}^x + S_n^y S_{n+1}^y\right), \tag{1}$$

can be transformed into a quadratic fermionic Hamiltonian through the Jordan–Wigner transformation[20], which allows to rewrite the initial spin Hamiltonian in terms of free spinless lattice fermions what provides a direct connection between spin and fermionic descriptions of one-dimensional quantum systems[21,22]. A special class of spin $S = 1/2$ chain models with multi-spin interactions, allowing an exact solution in terms of a *Fermi gas of spinless Fermions*, was proposed by M. Suzuki more than fifty years ago[23]. Similar to the standard spin $S = 1/2$ XX chain[21,24], Suzuki models can be rewritten in terms of free spinless fermions on a 1D lattice by means of the Jordan-Wigner transformation, but with long-distance hopping determined by the structure of the multi-spin term. As a result, Suzuki models provide a unique opportunity for realizing topological Lifshitz transitions in 1D[25] where, for a given band filling, the number of Fermi points changes with change of the multi-spin coupling.

In particular, cluster-XY models in which multispin cluster terms compete with nearest-neighbor XY exchange can still be mapped onto free fermionic systems and solved exactly, allowing their phase structure and quantum critical behavior to be determined analytically. These results demonstrate that the combination of conventional XY exchange with suitably structured cluster interactions provides an analytically tractable framework for investigating the effects of extended many-body interactions in quantum spin chains.

As a result, already decades ago the Suzuki model with three-spin iteraction has attracted considerable interest of researchers as a playground for studying topological quantum phase transitions in 1D[26–38]. The Suzuki chain provides a useful framework for investigating the effects of multispin interactions in one-dimensional quantum systems. By extending conventional nearest-neighbor exchange to include higher-order spin couplings, this class of models offers a route to exploring how multispin interactions modify quantum criticality and the structure of low-energy excitations. Recent developments in spin chains with four-spin cluster interactions have further highlighted the potential of these models for realizing topological phases and unconventional Lifshitz transitions.

A closely related class of models has recently been investigated by extending the spin-$1/2$ XY or XX chain with anisotropic four-spin cluster interactions[39–44]. These studies have demonstrated that multispin couplings can substantially enrich the ground-state properties of otherwise well-established one-dimensional spin models. In particular, anisotropic four-spin interactions in the XX chain have been shown to generate multiple gapped topological phases characterized by distinct winding numbers and characteristic entanglement-spectrum degeneracies[39]. Related investigations have further revealed that such four-spin interactions can give rise to nontrivial quantum-information signatures, including characteristic spin-squeezing behavior associated with symmetry-protected topological phases[40], as well as distinct entanglement and correlation landscapes involving concurrence, quantum discord, and entanglement entropy[41]. More recently, the interplay between four-spin interactions, exchange anisotropy, and external fields has been shown to produce higher-winding topological phases and several types of Lifshitz criticality associated with reconstructions of the Fermi-point structure[42]. The relation between Fermi-point topology and emergent conformal criticality has also been explored, revealing that the reconstruction of low-energy modes can lead to critical theories with different effective central charges[43].

Thermodynamic and magnetic anomalies emergent at the topological Livshitz transition, in the case of XX with four-spin interaction has been considered in the Ref.[44]. It has been shown that the flattering of the spinless-fermion spectrum at Fermi points, being manifestation of the Livshitz transition in terms of equivalent spinless-fermion model, determines the singular character of the density of states at transition and, as a consequence, unconventional temperature dependence of heat capacity and of the magnetic susceptibility of the system.

Collectively, these results establish the XY/XX chain with four-spin cluster interactions as a rich and analytically tractable platform for studying topology, quantum criticality, entanglement, and unconventional low-energy phenomena. The model considered in the present work reduces precisely to this previously studied four-spin XY/XX class in the limit $\Delta = 0$. This connection provides a natural starting point for investigating how the inclusion of the longitudinal $\Delta S_n^z S_{n+1}^z$ interaction modifies the phase structure and critical behavior of these previously established cluster-interaction models.

Despite the exact solvability of the XY and cluster-XY limits, these models describe only a restricted class of quantum spin systems because they neglect the longitudinal $S^z_n S^z_{n+1}$ exchange interaction. Such a longitudinal coupling is an intrinsic component of many realistic spin-$1/2$ systems and is particularly important in quasi-one-dimensional magnetic materials, where the low-energy physics is often described by anisotropic Heisenberg or XXZ spin chains. For example, the quasi-one-dimensional antiferromagnet $BaCo_2V_2O8$ is well described by an XXZ spin-chain Hamiltonian containing both transverse and longitudinal exchange interactions[45,46]. The same type of anisotropic spin interaction can also be engineered in ultracold atoms trapped in optical lattices, where effective XXZ couplings emerge from superexchange processes and their transverse and longitudinal components can be controlled experimentally[47–49]. Thus, the longitudinal interaction should not be regarded merely as a formal extension of the XY model. Its competition with the transverse exchange changes the energetic balance between different spin configurations and modifies the many-body correlations and quantum fluctuations of the system. In the fermionic representation, moreover, the $S^z_n S^z_{n+1}$ term generates interactions between the Jordan–Wigner fermions, thereby taking the model beyond the free-fermion structure that underlies the exact solution of the corresponding XY and cluster-XY limits. Investigating this term therefore provides a natural route toward understanding how the phase structure and critical properties of the exactly solvable cluster-XY model evolve when a physically relevant longitudinal interaction is introduced.

In the present work, we investigate the ground-state properties of the spin-$1/2$ XXZ chain with a four-spin interaction, focusing on the role of the longitudinal exchange term in modifying the phases previously identified in the $\Delta = 0$ limit. To provide a comprehensive characterization of the ground-state phase diagram, we employ three complementary approaches: Lanczos exact diagonalization, density-matrix renormalization group (DMRG)[50–52], and a fermionic mean-field treatment based on the Jordan–Wigner transformation[53]. Lanczos diagonalization enables us to obtain accurate ground-state properties and low-lying excitation spectra for finite chains, while DMRG allows us to access substantially larger system sizes and to investigate the ground-state properties in the thermodynamic regime. In parallel, the Jordan–Wigner mean-field approach provides an analytical description of the underlying fermionic quasiparticle spectrum and allows us to identify the conditions for gap closing, thereby providing useful insight into the location and nature of quantum phase transitions. By combining these complementary approaches, we examine the ground-state energy, spin correlations, entanglement-related quantities, and other characteristic observables as functions of the anisotropy parameter Δ and the four-spin coupling. Particular attention is devoted to identifying quantum phase transitions and determining how the longitudinal exchange interaction modifies the topology, criticality, and phase boundaries of the model. The comparison between the unbiased numerical results and the analytical mean-field description further allows us to assess the robustness of the phase boundaries and to clarify the physical mechanisms underlying the observed phase structure. Our results therefore provide a direct extension of the previously studied $\Delta = 0$ model and elucidate the role of the longitudinal exchange interaction in the ground-state physics of anisotropic four-spin quantum spin chains.

To further explore these aspects, the remainder of the paper is organized as follows. In Sec. 2, we introduce the model and discuss its relevant symmetries. In Sec. 3, we present and compare our results for the relevant order parameters and quantum fluctuations. Finally, in Sec. 4, we summarize our main findings and draw our conclusions.

2 The model

The Hamiltonian describing the 1D spin-1/2 XXZ model with isotropic four-spin interaction is expressed as:

$$\mathscr{H} = J\sum_{n=1}^{N}\left(S^x_n S^x_{n+1} + S^y_n S^y_{n+1} + \Delta S^z_n S^z_{n+1}\right) + J'\sum_{n=1}^{N}\left((S^x_n S^x_{n+3} + S^y_n S^y_{n+3})S^z_{n+1}S^z_{n+2}\right), \tag{2}$$

where S_n represents the spin operator at site n. The parameter $J > 0$ corresponds to the antiferromagnetic exchange coupling, while J' characterizes the strength of the four-spin interaction. The system size is given by N, representing the total number of spins. Periodic boundary conditions are assumed, ensuring that $S^\mu_{n+N} = S^\mu_n$, where μ takes values along the x, y, or z directions.

The Hamiltonian possesses several important symmetries. First, it is invariant under continuous rotations about the z axis, corresponding to a global $U(1)$ spin-rotation symmetry. The associated conserved quantity is the total z-component of spin,

$$S^z_{\text{tot}} = \sum_{n=1}^{N} S^z_n, \tag{3}$$

which satisfies

$$[\mathscr{H}, S^z_{\text{tot}}] = 0. \tag{4}$$

This conservation law allows the Hilbert space to be decomposed into independent sectors labeled by S^z_{tot}, which is particularly useful for the Lanczos exact-diagonalization calculations. In addition, the translational invariance of the Hamiltonian under

$n \to n+1$ follows from the periodic boundary conditions, so that the crystal momentum is also a good quantum number. The Hamiltonian is furthermore invariant under spatial reflection (parity), which maps $n \to N+1-n$, and under the global spin-flip transformation $S_n^z \to -S_n^z$, $S_n^{x,y} \to S_n^{x,y}$, corresponding to a $\mathbb{Z}_2$ symmetry. These symmetries constrain the structure of the ground-state and excitation spectra and provide useful quantum numbers for characterizing the different phases.

To investigate the ground-state properties and quantum phase behavior of the model, we employ three complementary approaches: Lanczos exact diagonalization, the DMRG, and a fermionic mean-field approximation based on the Jordan–Wigner transformation. In the following, we briefly describe each of these methods.

2.0.1 Lanczos exact diagonalization

For finite chains, we first employ the Lanczos exact diagonalization method to obtain the low-energy spectrum and the corresponding eigenstates of the Hamiltonian. The Hamiltonian is represented in the appropriate basis of the spin-$1/2$ Hilbert space, and the Lanczos algorithm is used to determine the lowest-energy eigenvalues and eigenvectors without requiring the full diagonalization of the Hamiltonian matrix. In particular, the ground-state energy E_0 and the corresponding ground-state wave function $|\psi_0\rangle$ are used to calculate various physical quantities, including the excitation gap, correlation functions, and order parameters. Since the Lanczos method treats the Hamiltonian directly, without relying on a mean-field decoupling or other approximations, it provides an accurate benchmark for finite system sizes. Its main limitation is the exponential growth of the Hilbert-space dimension with the system size, which restricts the maximum accessible chain length. Nevertheless, the method is particularly useful for analyzing the low-energy spectrum and for establishing a benchmark against which the DMRG and mean-field results can be compared.

2.0.2 Density-matrix renormalization group

To extend the analysis to larger system sizes and to reduce finite-size effects, we employ the DMRG method. DMRG is particularly well suited for 1D quantum spin systems, where the ground state can be efficiently represented in terms of a matrix-product state. During the iterative optimization procedure, the most relevant states are retained according to the eigenvalues of the reduced density matrix, while states with negligible contributions are discarded. The resulting optimized ground-state wave function is then used to calculate the ground-state energy and relevant observables, such as local magnetizations, correlation functions, and excitation gaps. In the present work, DMRG provides an independent numerical approach to the Lanczos calculations and allows us to investigate system sizes that are beyond the practical limits of exact diagonalization. Agreement between the Lanczos and DMRG results for overlapping system sizes serves as an important consistency check, while the larger system sizes accessible to DMRG allow a more reliable analysis of the behavior in the thermodynamic limit.

2.0.3 Jordan–Wigner mean-field approximation

As a complementary analytical approach, we transform the spin Hamiltonian into a fermionic representation using the Jordan–Wigner transformation. Under this transformation, the spin operators are expressed in terms of spinless fermionic creation and annihilation operators, allowing the original interacting spin model to be reformulated as an interacting fermionic Hamiltonian. The resulting higher-order fermionic terms are subsequently treated within a mean-field approximation by decoupling the interaction terms in terms of appropriate expectation values. This procedure leads to an effective quadratic fermionic Hamiltonian, which can be diagonalized to obtain the corresponding quasiparticle spectrum. The resulting spectrum provides analytical information about the gap-closing conditions and, consequently, the possible locations of quantum phase transitions. Although the mean-field treatment does not fully account for quantum correlations beyond the chosen decoupling scheme, it provides a useful analytical description of the low-energy fermionic structure of the model. In particular, it allows the numerical results obtained from Lanczos and DMRG to be interpreted in terms of the underlying fermionic quasiparticles and their gap-closing behavior. The predictions of the Jordan–Wigner mean-field approximation are therefore compared with the unbiased numerical results to assess the validity and physical implications of the analytical treatment.

3 Results

To obtain an initial insight into the ground-state phase diagram and a qualitative understanding of how the anisotropic interaction affects the ground-state phases of the system, we develop a fermionic mean-field description of the model. To this end, we employ the Jordan–Wigner transformation, which maps the spin-$1/2$ operators onto spinless fermionic operators. We adopt the following convention:

$$\begin{aligned} S_n^+ &= a_n^\dagger \exp\left(i\pi \sum_{j<n} a_j^\dagger a_j\right), \\ S_n^z &= a_n^\dagger a_n - \frac{1}{2}, \end{aligned} \tag{5}$$

where $a_n^\dagger$ and a_n are the fermionic creation and annihilation operators, respectively. Consequently, the fermionized interacting form of the Hamiltonian is obtained as

$$\mathscr{H} = \frac{J}{2}\sum_n \left(a_n^\dagger a_{n+1} + a_{n+1}^\dagger a_n\right) + J\Delta\sum_n \left(n_n - \frac{1}{2}\right)\left(n_{n+1} - \frac{1}{2}\right) + \frac{J'}{8}\sum_n \left(a_n^\dagger a_{n+3} + a_{n+3}^\dagger a_n\right). \quad (6)$$

In the next step, we use the mean-field approximation to decouple the interaction term, $a_n^\dagger a_n a_{n+1}^\dagger a_{n+1}$, leading to an approximate quadratic Hamiltonian. Wick's theorem is then employed to calculate the necessary quantities within this framework. We define the parameters, $\gamma_{i=1,2,3}$, as an expectation value of the fermionic two-point correlation functions[53,54],

$$\begin{aligned}\gamma_1 &= \langle a_n^\dagger a_n\rangle,\\ \gamma_2 &= \langle a_n^\dagger a_{n+1}\rangle,\\ \gamma_3 &= \langle a_n^\dagger a_{n+1}^\dagger\rangle,\end{aligned} \quad (7)$$

where the expectation values, $\langle ...\rangle$ are calculated in the ground state of the system. By utilizing these parameters and performing a Fourier transformation as $a_n = \frac{1}{\sqrt{N}}\sum_k e^{-ikn}a_k$, and also Bogoliubov transformation

$$a_k = \cos(\theta_k)\beta_k + i\sin(\theta_k)\beta_{-k}^\dagger, \quad (8)$$

the diagonalized Hamiltonian is obtained as

$$\mathscr{H} = \sum_k \varepsilon(k)(\beta_k^\dagger\beta_k - \frac{1}{2}). \quad (9)$$

The single-particle dispersion relation or the energy spectrum is given by

$$\varepsilon(k) = \sqrt{\mathscr{A}_k^2 + \mathscr{B}_k^2}, \quad (10)$$

with

$$\cos(\theta_k) = \frac{1}{\sqrt{2}}\sqrt{1 + \frac{\mathscr{A}_k}{\varepsilon(k)}}, \quad (11)$$

where

$$\begin{aligned}\mathscr{A}_k &= J\Delta(2\gamma_1 - 1) + J(1 - 2\Delta\gamma_2)\cos(k) + \frac{1}{4}J'\cos(3k),\\ \mathscr{B}_k &= 2J\Delta\gamma_3\sin(k).\end{aligned} \quad (12)$$

One should note that the following equations should be satisfied self-consistently:

$$\begin{aligned}\gamma_1 &= \frac{1}{2N}\sum_k(1 - \frac{\mathscr{A}_k}{\varepsilon(k)}),\\ \gamma_2 &= \frac{1}{2N}\sum_k\cos(k)(1 - \frac{\mathscr{A}_k}{\varepsilon(k)}),\\ \gamma_3 &= -\frac{i}{2N}\sum_k\cos(k)\frac{\mathscr{B}_k}{\varepsilon(k)} - \frac{1}{2N}\sum_k\sin(k)\frac{\mathscr{B}_k}{\varepsilon(k)}.\end{aligned} \quad (13)$$

In the limit $\Delta \to -\infty$, the system is driven into the classical ferromagnetic phase, characterized by $\gamma_1 = 1.0$, $\gamma_2 = \gamma_3 = 0$. In this limit, the corresponding single-particle dispersion relation reduces to

$$\varepsilon(k) = \Delta + \cos(k) + \frac{J'}{4}\cos(3k), \quad (14)$$

where we have set $J = 1$ as the energy scale without loss of generality. The critical value of Δ can be obtained from the condition for the closing of the excitation gap. Since the system is in the classical ferromagnetic phase for $\Delta \to -\infty$, the gap closes when the maximum of the dispersion relation reaches zero. From Eq. (14), we have

$$\max_k \varepsilon(k) = 0. \quad (15)$$

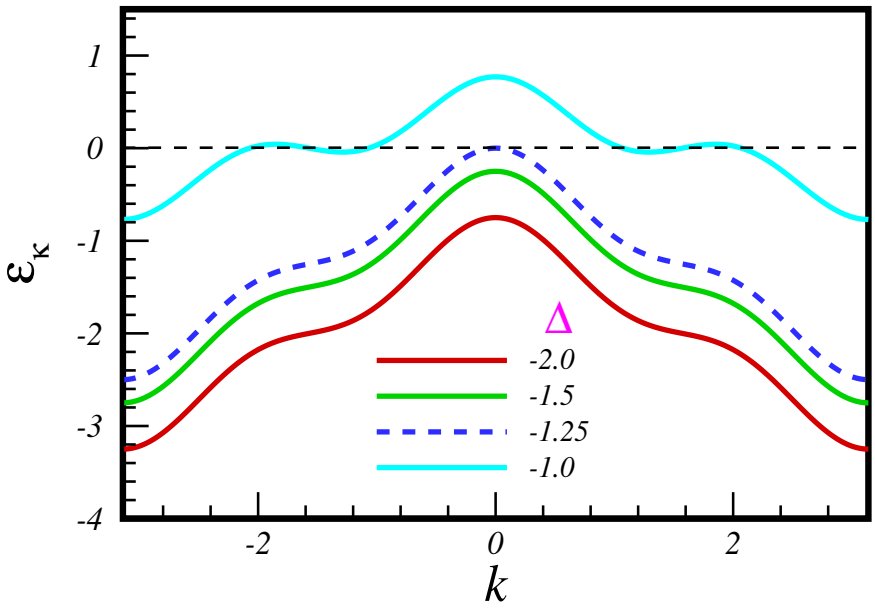

Figure 1. (color online). Dispersion relation obtained within the mean-field approximation for $J' = 1.0$ and a chain size of $N = 1000$, for three representative values of the anisotropy parameter, $\Delta = -2.0, -1.5, -1.25$, and -1.0. The progressive closing of the excitation gap upon approaching the critical value $\Delta_c = -1.25$ is clearly visible.

For $J' > 0$, the maximum of $\varepsilon(k)$ occurs at $k = 0$, yielding

$$\varepsilon(0) = \Delta + 1 + \frac{J'}{4}. \tag{16}$$

Consequently, the gap closes at

$$\Delta_{c_1} = -(1 + \frac{J'}{4}). \tag{17}$$

Thus, the transition out of the classical ferromagnetic phase occurs when the excitation gap closes at $k = 0$.

On the other hand, as the anisotropy parameter Δ is increased beyond the critical value Δ_{c_1}, the system undergoes a transition into a non-magnetic phase characterized by a vanishing magnetization. In this regime, the mean-field analysis yields the order parameters $\gamma_1 = 0.5$, $\gamma_3 = 0$, while γ_2 remains finite and generally depends on the anisotropy parameter Δ. Thus, in contrast to the magnetic phase below Δ_{c_1}, the dominant mean-field correlations in this region are associated with the second-neighbor channel, whereas the third-neighbor contribution vanishes. The corresponding single-particle dispersion relation provides further insight into the nature of this phase. In particular, the spectrum becomes gapless at multiple momenta, giving rise to six Fermi points within the first Brillouin zone. Two of these points are fixed at

$$k_f = \pm\frac{\pi}{2},$$

while the remaining four are determined by

$$\sin(k_F) = \pm\sqrt{\frac{1}{4} + \frac{1 - 2\Delta\gamma_2}{J'}}.$$

Therefore, the Fermi-point structure consists of the two fixed crossings at $\pm\pi/2$ together with two pairs of additional crossings whose positions continuously depend on Δ, γ_2, and the strength of the four-spin interaction J'. The appearance of these six Fermi points indicates that the low-energy spectrum in this parameter regime is considerably richer than that of a conventional two-Fermi-point phase. In particular, the evolution of the additional Fermi points with Δ provides a useful way of characterizing the underlying changes in the low-energy structure and the associated quantum phase transition.

It is important to emphasize that the present Jordan–Wigner mean-field treatment is primarily suited to describing the instability of the large-negative-Δ ferromagnetic regime and does not fully capture the physics of the large-positive-Δ region. In the latter limit, the system approaches a Néel-ordered state characterized by a staggered magnetization, $\langle S_n^z \rangle \propto (-1)^n$, which, in the Jordan–Wigner representation, corresponds to a staggered fermionic density, $\langle n_n \rangle \neq \langle n_{n+1} \rangle$. The mean-field ansatz employed here assumes translationally invariant correlation parameters, in particular a site-independent density $\gamma_1 = \langle n_n \rangle$, and therefore does not allow for such a two-sublattice structure. Consequently, the gap-closing condition obtained from the present mean-field dispersion reliably characterizes the instability of the ferromagnetic phase, but it does not reproduce the critical boundary associated with the Néel regime at positive Δ. The phase boundaries in this region are therefore determined from the unbiased Lanczos and DMRG calculations, which do not impose translationally invariant mean-field order parameters.

In Fig. 1, we present the single-particle dispersion relation obtained within the mean-field approximation for $J' = 1.0$, four representative values of the anisotropy parameter, $\Delta = -2.0$, -1.5, -1.25, and -1.0, and a chain size of $N = 1000$. The evolution of the dispersion with increasing Δ clearly illustrates the change in the low-energy structure of the system across the critical point. For $\Delta = -2.0$ and $\Delta = -1.5$, the excitation spectrum is fully gapped, indicating that the system is in a non-critical regime. In both cases, the dispersion exhibits a pronounced maximum around $k = 0$, while the excitation energy remains finite throughout the Brillouin zone. As Δ is increased from -2.0 toward the critical region, the minimum excitation energy decreases continuously, and the gap becomes progressively smaller. This continuous suppression of the gap signals that the system is approaching a quantum critical point.

At the critical value $\Delta = \Delta_{c_1} = -1.25$, the excitation gap closes, marking the onset of a qualitatively different low-energy structure. The closing of the gap indicates that low-energy excitations become gapless at specific momenta and, consequently, that the system reaches a critical point separating two distinct spectral regimes. Upon further increasing the anisotropy to $\Delta = -1.0$, the spectrum becomes clearly gapless over several isolated momenta. Most notably, exactly six Fermi points can be identified in the first Brillouin zone. These points correspond to the momenta at which the single-particle excitation energy vanishes and therefore determine the low-energy modes of the system. The emergence of six Fermi points, in contrast to the gapped spectra observed for $\Delta < \Delta_{c_1}$, provides a direct signature of the reconstructed low-energy spectrum in the non-magnetic phase. Thus, Fig. 1 demonstrates how increasing Δ drives a continuous closing of the excitation gap at Δ_{c_1}, followed by the formation of a six-Fermi-point gapless structure for $\Delta > \Delta_{c_1}$.

To obtain a reliable characterization of the ground-state phase diagram beyond the limitations of the mean-field approximation, we next turn to unbiased numerical calculations. In the following, we present the results obtained from Lanczos exact diagonalization and DMRG calculations. By combining these two complementary numerical approaches, we determine the phase boundaries and characterize the different ground-state regimes, including the critical region at positive Δ that is not explicitly captured by the translationally invariant mean-field ansatz.

We begin our numerical investigation by analyzing the ground-state energy density,

$$e_g = \frac{E_g}{N}$$

where E_g denotes the ground-state energy of a chain of length N. Exact diagonalization based on the Lanczos algorithm is performed for relatively small systems with $N = 12$, 16, 20, and 24, while larger systems with $N = 40$ and 60 are investigated using the DMRG method. We consider a broad range of the anisotropy parameter Δ and different values of the exchange couplings. For clarity, and because the qualitative behavior remains unchanged, in the following we restrict our discussion to the representative case $J = 1$ and $J' = 1$.

Figure 2 (a) shows the ground-state energy density e_g as a function of the anisotropy parameter Δ for the different system sizes. A remarkable feature of the results is the very weak dependence of e_g on the system size over the entire parameter range considered. The data obtained from the Lanczos and DMRG calculations practically follow the same curve, indicating that finite-size corrections to the ground-state energy density are relatively small. Moreover, e_g remains negative throughout the investigated range of Δ. As Δ is increased, however, a clear nonanalytic behavior develops at the first critical point, Δ_{c_1}, where the classical ferromagnetic phase gives way to the gapless phase identified from the mean-field analysis.

To characterize this transition more clearly, in Fig. 2 (b) we plot the first derivative of the ground-state energy density, $e_g' = \partial e_g / \partial \Delta$, as a function of Δ. The transition is manifested by a pronounced discontinuity or rapid change in the derivative at Δ_{c_1}. This behavior provides a direct indication of the nonanalyticity of the ground-state energy and is consistent with the first-order character of the transition between the FM and gapless phases. In contrast to the ground-state energy density itself, the derivative exhibits a much more pronounced sensitivity to the system size, although the corresponding finite-size effects remain relatively weak. The crossing or convergence of the results for different system sizes allows us to estimate the thermodynamic-limit location of the transition. By analyzing the size dependence of the numerical data and extrapolating the corresponding finite-size estimates to the thermodynamic limit, we obtain

$$\Delta_{c_1} \simeq -1.21,$$

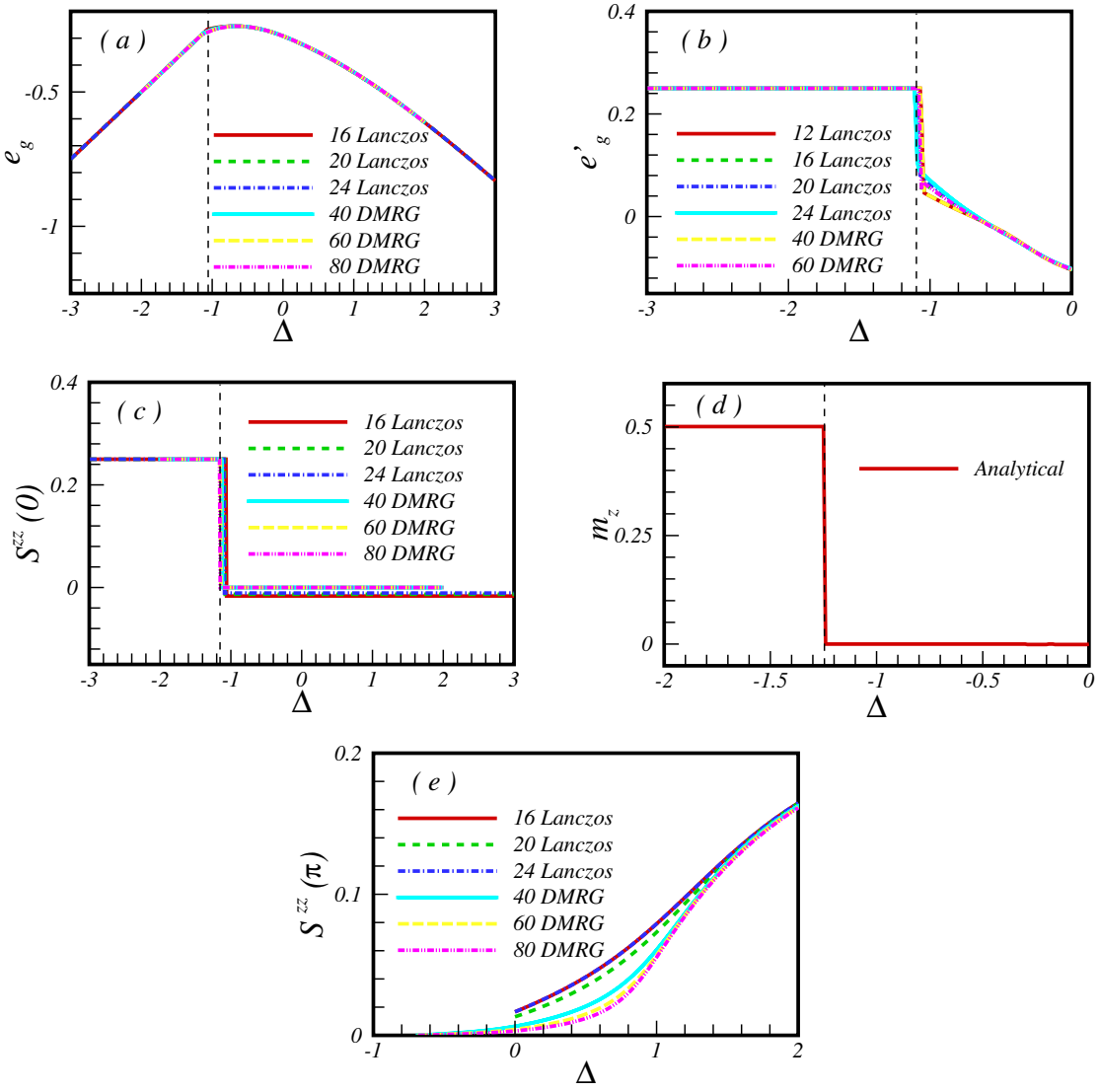

Figure 2. (color online). (a) Ground-state energy density e_g, (b) its first derivative with respect to Δ, (c) longitudinal spin structure factor $S^{zz}(q=0)$, (d) longitudinal magnetization m^z, and (e) longitudinal spin structure factor $S^{zz}(q=\pi)$, as functions of the anisotropy parameter Δ, for $J = J' = 1$. The results are obtained using Lanczos exact diagonalization for $N = 16$ and 20, and DMRG for $N = 40$, 60, and 80.

which is reasonably close to the analytical mean-field prediction,

$$\Delta_{c_1}^{\mathrm{MF}} = -1.25.$$

The small difference between the numerical and analytical estimates can be attributed to finite-size effects and, more importantly, to the approximate nature of the mean-field treatment. Nevertheless, the overall agreement between the numerical calculations and the analytical prediction supports the identification of Δ_{c_1} as the boundary between the ferromagnetic and gapless regimes. The combined behavior of e_g and its first derivative therefore provides an independent numerical confirmation of the phase boundary obtained from the mean-field analysis.

In the ground state phase diagram, the ferromagnetic phase is prevalent in the region where $\Delta < \Delta_{c_1}$. This phase is characterized by all spins aligning in the z direction, a consequence of the dominant ferromagnetic exchange interaction. The uniform magnetization observed in this phase is defined by the equation:

$$m^z = \frac{1}{N}\sum_{n=1}^{N}\langle S_n^z\rangle. \tag{18}$$

It should be noted that the spin structure factor also gives us a deep insight into the characteristics of the ground state. It is defined as

$$S^{zz}(q) = \frac{1}{N-1}\sum_{m=1}^{N-1} e^{iqm}\langle S_n^z S_{n+m}^z\rangle. \tag{19}$$

Notably, the spin structure factor at $q=0$ signifies ferromagnetic ordering, while at $q=\pi$, it reveals Néel long-range order within the ground state phase diagram.

To further characterize the magnetic properties of the different phases and to provide an independent numerical signature of the phase boundaries, we calculate the longitudinal spin structure factor S^{zz}. The results for different system sizes are presented in Fig. 2 (c) as a function of the anisotropy parameter Δ. A clear distinction between the ferromagnetic and gapless regimes can be observed. In the ferromagnetic region, quantum fluctuations in the longitudinal spin component are absent, and the spin structure factor takes its saturated value,

$$S^{zz}(0) = \frac{1}{4}.$$

This value is independent of the system size within the numerical accuracy and remains essentially constant throughout the ferromagnetic phase.

Upon increasing Δ and crossing the first critical point Δ_{c_1}, the behavior of S^{zz} changes abruptly. As the system enters the gapless phase, the longitudinal magnetic order is rapidly suppressed and $S^{zz}(0)$ decreases from its saturated ferromagnetic value. In this regime, quantum fluctuations become important and destroy the long-range ferromagnetic polarization present in the ferromagnetic phase. Accordingly, $S^{zz}(0)$ remains very small throughout the gapless region. Importantly, its value is not exactly zero for finite systems, reflecting residual quantum fluctuations and finite-size effects. The progressive suppression of $S^{zz}(0)$ therefore provides an additional indication of the transition from the fully polarized ferromagnetic state to the non-magnetic gapless phase.

The behavior of the longitudinal magnetization provides a complementary characterization of this transition. In Fig. 2 (d), we plot the magnetization along the z direction obtained from our analytical mean-field results. The analytical magnetization decreases from its saturated value in the ferromagnetic region and vanishes upon entering the gapless phase. Remarkably, the analytical prediction shows excellent agreement with the numerical behavior of $S^{zz}(0)$ shown in Fig. 2 (c). In particular, both quantities identify almost the same phase boundary at Δ_{c_1} and consistently distinguish the fully polarized FM phase from the non-magnetic gapless regime.

The simultaneous behavior of $S^{zz}(0)$ and the longitudinal magnetization thus provides an important consistency check between the numerical calculations and the analytical mean-field treatment. While the ground-state energy characterizes the energetic evolution across the transition, the spin structure factor directly probes the magnetic character of the ground state. Their combined behavior confirms that the phase for $\Delta < \Delta_{c_1}$ is fully polarized, whereas for $\Delta > \Delta_{c_1}$ the system enters a fluctuation-dominated gapless phase with vanishing magnetization in the thermodynamic limit.

Finally, in Fig. 2 (e), we present the numerical results for the spin structure factor at momentum $q=\pi$, $S^{zz}(\pi)$, which provides a direct probe of staggered longitudinal spin correlations and is therefore particularly relevant for identifying the possible emergence of N'eel order. In the absence of the four-spin interaction, i.e., for $J'=0$, the standard XXZ chain develops a N'eel ordered phase for $\Delta > \Delta_{c_2} = 1$. This naturally suggests that, for finite J', the gapless phase may eventually give way to a N'eel phase at a second critical point, which we denote by $\Delta = \Delta_{c_2}(J')$. As shown in Fig. 2 (e), $S^{zz}(\pi)$ vanishes in the ferromagnetic region, $\Delta < \Delta_{c_1}$, where the spins are uniformly polarized and staggered correlations are absent. Upon entering the gapless phase, $S^{zz}(\pi)$ remains very small over an extended range of Δ, reflecting the absence of long-range N'eel order and the dominance of quantum fluctuations. As the anisotropy becomes positive and is further increased, however, $S^{zz}(\pi)$ starts to increase and exhibits a smooth, approximately monotonic growth, indicating an enhancement of antiferromagnetic correlations at momentum $q=\pi$. Despite this clear tendency toward staggered ordering, no pronounced anomaly or sharp feature associated with the second critical point $\Delta_{c_2}(J')$ is visible in $S^{zz}(\pi)$ for the system sizes considered. This behavior indicates that, although the staggered structure factor captures the gradual development of antiferromagnetic correlations, it is not sufficiently sensitive to provide a reliable determination of the second critical point from finite-size data alone. The absence of a clear singularity should therefore not be interpreted as evidence for the absence of the N'eel transition; rather, it motivates the use of more sensitive observables to locate $\Delta_{c_2}(J')$.

The absence of a pronounced signature of the second critical point in our finite-size numerical results deserves some discussion. As a useful reference, we recall the well-known behavior of the one-dimensional antiferromagnetic XXZ chain, where the transition at $\Delta = 1$ separates the gapless Luttinger-liquid phase from the gapped N'eel phase. This transition is of Berezinskii–Kosterlitz–Thouless (BKT) type and is characterized by an exceptionally weak finite-size signature. In particular, the excitation gap on the gapped side opens exponentially slowly, $\Delta_{\text{gap}} \sim \exp\left[-\frac{b}{\sqrt{\Delta-1}}\right]$, while the corresponding

correlation length grows exponentially as the transition is approached, $\xi \sim \exp\left[\frac{b'}{\sqrt{\Delta-1}}\right]$, where b and b' are positive constants. Consequently, very large system sizes may be required to distinguish the asymptotic gapped behavior from the critical one. This explains why neither the ground-state energy nor conventional two-point spin correlations necessarily exhibit a pronounced anomaly near a BKT transition in finite systems.

A similar situation can arise in the present model in the presence of the four-spin cluster interaction. Although this interaction modifies the low-energy spectrum, shifts the location of the critical point, and changes the effective parameters governing the low-energy correlations, the finite-size difficulty associated with a possible LL-to-gapped transition remains. In particular, if the second transition $\Delta_{c_2}(J')$ has BKT-like or marginal character, the associated correlation length may become much larger than the system sizes accessible to exact diagonalization. The finite chains can therefore display smooth variations in the ground-state energy and correlation functions even when the thermodynamic system crosses a genuine phase boundary. This behavior is qualitatively different from the first transition at Δ_{c_1}, where a pronounced change in the ground-state energy and its derivative provides a clear numerical signature.

To obtain a more sensitive characterization of the second critical point, we complement the conventional thermodynamic and spin-correlation functions with two quantum-information measures, namely the concurrence and quantum discord (QD)[55–59,59–62]. These measures provide a direct probe of the internal quantum structure of the ground state and can capture changes in short- and intermediate-range quantum correlations that may not be clearly reflected in conventional observables. In particular, pairwise entanglement, quantified by the concurrence, and QD have been extensively employed to identify quantum critical points through their extrema, discontinuities, or nonanalytic behavior, as well as through corresponding features in their derivatives[55,63–75]. We therefore analyze these quantities to identify signatures of the second critical point and obtain a more reliable estimate of $\Delta_{c_2}(J')$.

For a pair of spins located at sites i and j, the reduced density matrix is obtained by tracing out all other degrees of freedom,

$$\rho_{ij} = \mathrm{Tr}_{\overline{ij}}(\rho)\,, \tag{20}$$

where $\rho = |\psi_0\rangle\langle\psi_0|$ is the ground-state density matrix and $\mathrm{Tr}_{\overline{ij}}$ denotes the trace over the remaining spins. For the spin model considered here, the symmetries of the Hamiltonian lead to an X-type reduced density matrix in the standard basis $|00\rangle, |01\rangle, |10\rangle, |11\rangle$,

$$\rho_{i,j} = \begin{pmatrix} \langle p_i^{\uparrow} p_j^{\uparrow}\rangle & 0 & 0 & \langle S_i^- S_j^-\rangle \\ 0 & \langle p_i^{\uparrow} p_j^{\downarrow}\rangle & \langle S_i^- S_j^+\rangle & 0 \\ 0 & \langle S_i^+ S_j^-\rangle & \langle p_i^{\downarrow} p_j^{\uparrow}\rangle & 0 \\ \langle S_i^+ S_j^+\rangle & 0 & 0 & \langle p_i^{\downarrow} p_j^{\downarrow}\rangle \end{pmatrix}, \tag{21}$$

where the brackets denote the physical state average, and $p^{\uparrow} = \frac{1}{2} + S^z$, $p^{\downarrow} = \frac{1}{2} - S^z$, $S^{\pm} = S^x \pm iS^y$. In particular, the two-spin correlations entering the reduced density matrix are calculated directly from the ground-state wave function obtained by numerical Lanczos diagonalization method and DMRG.

The concurrence provides a measure of the pairwise entanglement between the two spins. For a general two-qubit state, it is defined as

$$C_{ij} = \max\{0, \lambda_1 - \lambda_2 - \lambda_3 - \lambda 4\}, \tag{22}$$

where $\lambda_1 \geq \lambda_2 \geq \lambda_3 \geq \lambda_4$ are the square roots of the eigenvalues of

$$R = \rho_{ij}\,(\sigma^y \otimes \sigma^y)\,\rho_{ij}^{\star}\,(\sigma^y \otimes \sigma^y)\,. \tag{23}$$

The concurrence ranges from zero, corresponding to a separable two-spin state, to unity for a maximally entangled pair. Thus, changes in C_{ij} can reveal modifications of the local entanglement structure across a quantum phase transition.

As a complementary measure, we also calculate the QD, which quantifies quantum correlations beyond entanglement and can remain finite even for mixed states with zero concurrence. The quantum mutual information is defined as

$$I(\rho_{ij}) = S(\rho_i) + S(\rho_j) - S(\rho_{ij}), \tag{24}$$

where

$$S(\rho) = -\mathrm{Tr}(\rho \log_2 \rho) \tag{25}$$

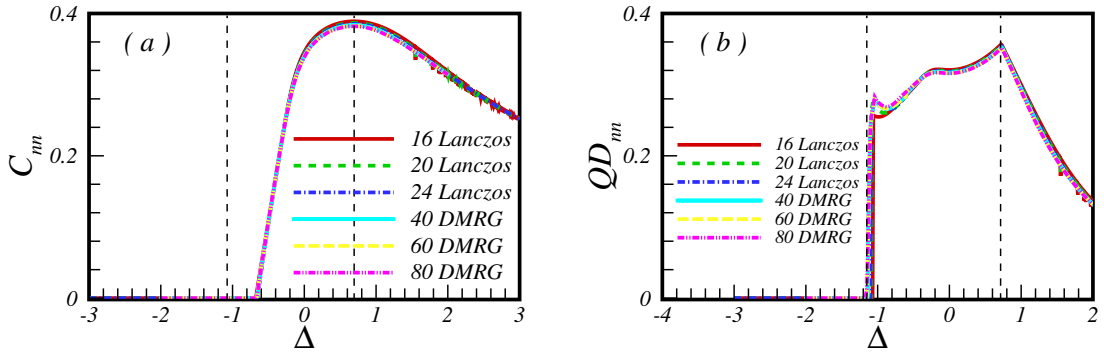

Figure 3. (color online). (a) Nearest-neighbor concurrence $C_{i,i+1}$ and (b) nearest-neighbor quantum discord $QD_{i,i+1}$ as functions of the anisotropy parameter Δ, for $J = J' = 1$. The results are obtained using Lanczos exact diagonalization for $N = 16$ and 20, and DMRG for $N = 40$, 60, and 80.

is the von Neumann entropy and $\rho_i = \mathrm{Tr}_j(\rho_{ij})$ and $\rho_j = \mathrm{Tr}_i(\rho_{ij})$ are the corresponding one-spin reduced density matrices. The classical correlation is obtained by optimizing the conditional entropy over local measurements on one of the two spins,

$$J(\rho_{ij}) = S(\rho_i) - \min_{\Pi_k^j} \sum_k p_k S(\rho_{i|k}), \tag{26}$$

where Π_k^j denotes a complete set of local projective measurements on spin j. The QD is then given by

$$QD_{ij} = I(\rho_{ij}) - J(\rho_{ij}). \tag{27}$$

Unlike concurrence, quantum discord is not restricted to entanglement and can capture a broader class of nonclassical correlations.

In the following, we evaluate C_{ij} and QD_{ij} between nearest neighbour pair spins as functions of the anisotropy parameter Δ for different system sizes. Particular attention is paid to the nearest-neighbor correlations, for which these quantities are expected to provide a sensitive probe of changes in the ground-state structure. Their behavior is subsequently used to identify the critical region associated with the second transition and to estimate $\Delta_{c_2}(J')$.

The numerical results for the concurrence and QD between nearest-neighbor spin pairs are presented in Fig. 3. These quantum-information measures provide a more sensitive characterization of the changes in the ground-state structure across the different phases. In the ferromagnetic phase, $\Delta < \Delta_{c_1}$, the ground state is fully polarized and the nearest-neighbor spins are in a separable state. Consequently, both the concurrence and the QD associated with the nearest-neighbor pair vanish in this region, indicating the absence of nonclassical correlations between the two spins. Upon crossing the first critical point and entering the gapless phase, the concurrence initially remains zero over a finite interval of Δ, as shown in Fig. 3 (a). With further increase of the anisotropy, however, quantum fluctuations become sufficiently strong to generate pairwise entanglement between neighboring spins. The concurrence then becomes finite and increases continuously with Δ, reaching a pronounced maximum at $\Delta_{c_2}(J' = 1) \simeq 0.73$. This maximum provides a clear signature of the second critical point and is particularly noteworthy because no comparable feature was observed in the conventional ground-state energy or in the staggered structure factor. Beyond Δ_{c_2}, the concurrence decreases as the system enters the N'eel phase. For sufficiently large positive Δ, the nearest-neighbor concurrence is strongly suppressed and tends toward zero, consistent with the increasing dominance of the Ising-like antiferromagnetic interaction and the approach to a classical N'eel state. Thus, the nonmonotonic behavior of the concurrence, with a maximum at Δ_{c_2}, provides a useful indication of the change from the gapless regime to the N'eel phase.

A particularly clear signature of both critical points is obtained from the quantum discord, shown in Fig. 3 (b). In contrast to concurrence, which measures only pairwise entanglement, QD captures a broader class of nonclassical correlations and can therefore remain finite even when the concurrence vanishes. In the ferromagnetic phase, the QD is essentially zero, reflecting the classical and separable nature of the fully polarized ground state. At the first critical point, Δ_{c_1}, the QD exhibits a pronounced jump, signaling the sudden development of nonclassical correlations as the system leaves the ferromagnetic phase and enters the fluctuation-dominated gapless regime. As Δ is increased further, the QD evolves smoothly within the gapless phase and develops a distinct cusp at $\Delta_{c_2}(J' = 1) \simeq 0.73$. The coincidence of this cusp with the position of the maximum of the concurrence provides independent evidence for the second critical point. Therefore, while conventional thermodynamic quantities and the staggered spin structure factor do not display a sufficiently sharp finite-size signature of the

second transition, the quantum-information measures reveal pronounced changes in the local quantum-correlation structure at both phase boundaries. In particular, the behavior of the QD offers a sensitive numerical criterion for locating Δ_{c_2} in the present finite-size systems.

4 Conclusion

In this work, we have investigated the ground-state phase structure of a one-dimensional spin-$1/2$ XXZ chain with four-spin cluster interactions by combining exact diagonalization Lanczos, DMRG calculations, and an analytical mean-field approach. By examining the ground-state energy, its derivative, the longitudinal spin correlations, the staggered spin structure factor, and the magnetization, we have characterized the evolution of the system with the anisotropy parameter and identified three distinct regimes: a ferromagnetic phase, an intermediate gapless phase, and a N'eel phase.

The first transition, separating the ferromagnetic and gapless phases, is clearly reflected in the ground-state energy and its derivative, as well as in the longitudinal spin correlations and magnetization. In contrast, the second transition, associated with the onset of the N'eel phase, does not produce an equally pronounced signature in the conventional finite-size observables considered here. In particular, the smooth behavior of the ground-state energy and the staggered spin structure factor makes it difficult to determine the second critical point accurately using these quantities alone. This difference highlights the importance of employing complementary observables when investigating phase transitions in interacting quantum spin systems.

To address this issue, we have examined the nearest-neighbor concurrence and QD as complementary probes of the ground-state quantum correlations. The concurrence exhibits a pronounced maximum near the second critical point, while the QD displays distinct features at both transitions, including a jump at the first critical point and a cusp near the second. For the representative cluster coupling $J' = 1$, these signatures indicate a second critical point at approximately $\Delta_{c_2} \simeq 0.73$. The different responses of concurrence and QD also illustrate their complementary roles: concurrence characterizes pairwise entanglement, whereas QD captures a broader class of nonclassical correlations.

Overall, our results demonstrate that quantum-information measures can provide useful signatures of phase transitions that are difficult to identify from conventional finite-size quantities. The present study therefore establishes a complementary approach to characterizing the phase structure of spin chains with multispin interactions. Further investigations of larger systems, finite-size scaling, and additional correlation measures would help refine the critical-point estimates and clarify the nature of the second transition.

Author contributions

M. A. performed the numerical simulations, analyzed the data, and prepared the figures. S. M. carried out the analytical calculations. M. A. also drafted the initial version of the manuscript. S. M. and G. I. J. contributed to the development of the theoretical framework and methodology, supervised the research, and provided scientific guidance. They also contributed to the validation of the results, the interpretation of the findings, and the discussion of their physical implications. S. M. and G. I. J. critically reviewed and edited the manuscript. All authors reviewed and approved the final version of the manuscript.

Competing interests

The authors declare no competing interests.

Data availability

The data sets used and/or analyzed during the current study are available from the corresponding author upon reasonable request

Funding

This research received no specific grant from any funding agency in the public, commercial, or not-for-profit sectors.

References

1. A. Furrer and O. Waldmann, "Magnetic cluster excitations," *Reviews of Modern Physics*, vol. 85, no. 1, pp. 367–420, 2013.
2. M. Podewitz and M. Reiher, "Spin interactions in cluster chemistry," *Advances in Inorganic Chemistry*, vol. 62, p. 177, 2010.
3. F. C. Alcaraz, R. A. Pimenta, and J. Sirker, "Ising analogs of quantum spin chains with multispin interactions," *Physical Review B*, vol. 107, no. 23, p. 235136, 2023.

4. N. Chancellor, S. Zohren, and P. A. Warburton, "Circuit design for multi-body interactions in superconducting quantum annealing systems with applications to a scalable architecture," *npj Quantum Information*, vol. 3, no. 1, p. 21, 2017.

5. T. Griffin and S. D. Bartlett, "Spin lattices with two-body hamiltonians for which the ground state encodes a cluster state," *Physical Review A—Atomic, Molecular, and Optical Physics*, vol. 78, no. 6, p. 062306, 2008.

6. R. Coldea, S. Hayden, G. Aeppli, T. Perring, C. Frost, T. Mason, S.-W. Cheong, and Z. Fisk, "Spin waves and electronic interactions in la 2 cuo 4," *Physical review letters*, vol. 86, no. 23, p. 5377, 2001.

7. S. Brehmer, H.-J. Mikeska, M. Müller, N. Nagaosa, and S. Uchida, "Effects of biquadratic exchange on the spectrum of elementary excitations in spin ladders," *Physical Review B*, vol. 60, no. 1, p. 329, 1999.

8. M. Matsuda, K. Katsumata, R. Eccleston, S. Brehmer, and H.-J. Mikeska, "Magnetic excitations and exchange interactions in the spin-1 2 two-leg ladder compound la 6 ca 8 cu 24 o 41," *Physical Review B*, vol. 62, no. 13, p. 8903, 2000.

9. S. Notbohm, P. Ribeiro, B. Lake, D. Tennant, K. Schmidt, G. Uhrig, C. Hess, R. Klingeler, G. Behr, B. Büchner, *et al.*, "One-and two-triplon spectra of a cuprate ladder," *Physical review letters*, vol. 98, no. 2, p. 027403, 2007.

10. W. Chunlei, Q. Zikai, and Z. Jingbo, "Green's function theory of phase transition in pbhpo4 and pbdpo4 ferroelectrics," *Ferroelectrics*, vol. 77, no. 1, pp. 21–29, 1988.

11. C. Wang, Z. Qin, and D. Lin, "Critical behavior of the ising model with four-spin coupling," *Journal of magnetism and magnetic materials*, vol. 88, no. 1-2, pp. 87–92, 1990.

12. C. Wang, Z. Qin, and D. Lin, "First-order phase transition in order-disorder ferroelectrics," *Physical Review B*, vol. 40, no. 1, p. 680, 1989.

13. C. Wang, Z. Qin, and D. Lin, "A microscopic model of first order phase transition in squaric acid," *Solid state communications*, vol. 71, no. 1, pp. 45–48, 1989.

14. M. Greiner, O. Mandel, T. Esslinger, T. W. Hänsch, and I. Bloch, "Quantum phase transition from a superfluid to a mott insulator in a gas of ultracold atoms," *nature*, vol. 415, no. 6867, pp. 39–44, 2002.

15. Z. Zhou, E. Zhao, and W. V. Liu, "Spin-orbital exchange of strongly interacting fermions in the p band of a two-dimensional optical lattice," *Physical Review Letters*, vol. 114, no. 10, p. 100406, 2015.

16. F. D. M. Haldane, "Nonlinear field theory of large-spin heisenberg antiferromagnets: Semiclassically quantized solitons of the one-dimensional easy-axis néel state," *Physical review letters*, vol. 50, no. 15, p. 1153, 1983.

17. S. Sachdev and B. Keimer, "Quantum criticality," *Physics Today*, vol. 64, no. 2, pp. 29–35, 2011.

18. X.-G. Wen, "Colloquium: Zoo of quantum-topological phases of matter," *Reviews of Modern Physics*, vol. 89, no. 4, p. 041004, 2017.

19. R. Moessner and J. E. Moore, "Topological phases of matter," *American history*, vol. 1861, no. 1900, 1945.

20. P. Jordan and E. Wigner, "Über das paulische äquivalenzverbot," *Zeitschrift für Physik*, vol. 47, no. 9, pp. 631–651, 1928.

21. E. Lieb, T. Schultz, and D. Mattis, "Two soluble models of an antiferromagnetic chain," *Annals of Physics*, vol. 16, no. 3, pp. 407–466, 1961.

22. M. Takahashi *et al.*, "Thermodynamics of one-dimensional solvable models," 1999.

23. M. Suzuki, "Equivalence of the two-dimensional ising model to the ground state of the linear xy-model," *Physics Letters A*, vol. 34, no. 2, pp. 94–95, 1971.

24. S. Katsura, "Statistical mechanics of the anisotropic linear heisenberg model," *Physical Review*, vol. 127, no. 5, p. 1508, 1962.

25. I. Lifshitz *et al.*, "Anomalies of electron characteristics of a metal in the high pressure region," *Sov. Phys. JETP*, vol. 11, no. 5, pp. 1130–1135, 1960.

26. D. Gottlieb and J. Rössler, "Exact solution of a spin chain with binary and ternary interactions of dzialoshinsky-moriya type," *Physical Review B*, vol. 60, no. 13, p. 9232, 1999.

27. I. Titvinidze and G. Japaridze, "Phase diagram of the spin extended model," *The European Physical Journal B-Condensed Matter and Complex Systems*, vol. 32, no. 3, pp. 383–393, 2003.

28. P. Lou, W.-C. Wu, and M.-C. Chang, "Quantum phase transition in spin-1 2 xx heisenberg chain with three-spin interaction," *Physical Review B—Condensed Matter and Materials Physics*, vol. 70, no. 6, p. 064405, 2004.

29. A. Zvyagin, "Quantum phase transitions in low-dimensional quantum spin systems with incommensurate magnetic structures," *Physical Review B—Condensed Matter and Materials Physics*, vol. 72, no. 6, p. 064419, 2005.

30. A. Zvyagin and G. Skorobagat'Ko, "Exactly solvable quantum spin model with alternating and multiple spin exchange interactions," *Physical Review B—Condensed Matter and Materials Physics*, vol. 73, no. 2, p. 024427, 2006.

31. T. Krokhmalskii, O. Derzhko, J. Stolze, and T. Verkholyak, "Dynamic properties of the spin-1 2 xy chain with three-site interactions," *Physical Review B—Condensed Matter and Materials Physics*, vol. 77, no. 17, p. 174404, 2008.

32. M. Topilko, O. Derzhko, and T. Krokhmalskii, "Dynamic properties of spin-1/2 xx chain with three-site interactions of (xzy-yzx)-type," *Acta Physica Polonica A*, vol. 119, no. 6, pp. 868–870, 2011.

33. M. Topilko, T. Krokhmalskii, O. Derzhko, and V. Ohanyan, "Magnetocaloric effect in spin-1/2 xx chains with three-spin interactions," *The European Physical Journal B*, vol. 85, no. 8, p. 278, 2012.

34. Y.-T. Sha, Y. Wang, Z.-H. Sun, and X.-W. Hou, "Thermal quantum coherence and correlation in the extended xy spin chain," *Annals of Physics*, vol. 392, pp. 229–241, 2018.

35. S. Yin, J. Song, S. Liu, and G. Song, "Quantum coherence and topological quantum phase transitions in the extended xy chain," *Physics Letters A*, vol. 389, p. 127089, 2021.

36. K. Cao, M. Zhong, and P. Tong, "Dynamical quantum phase transition in xy chains with the dzyaloshinskii-moriya and xzy–yzx three-site interactions," *Chinese Physics B*, vol. 31, no. 6, p. 060505, 2022.

37. S. Mahdavifar, K. Afrousheh, *et al.*, "Entangled unique coherent line in the ground-state phase diagram of the spin-1/2 xx chain model with three-spin interaction.," *Physical review. E*, vol. 109, no. 4-1, pp. 044142–044142, 2024.

38. R. K. Malakar and A. K. Ghosh, "Quantum phases of spin-1/2 extended xy model in transverse magnetic field," *Physica Scripta*, vol. 99, no. 3, p. 035944, 2024.

39. S. Mahdavifar and F. K. Fumani, "Topological phases driven by anisotropic four-spin interactions in 1d spin-1/2 xx chains," *Annalen der Physik*, vol. 538, no. 1, p. e00435, 2026.

40. F. Valeh and S. Mahdavifar, "Spin squeezing as a probe of symmetry-protected topological phases in an anisotropic four-spin cluster interaction," *Journal of Magnetism and Magnetic Materials*, p. 174459, 2026.

41. S. Mahdavifar, F. K. Fumani, and M. Soltani, "Chiral entanglement landscapes: Insights from a four-spin interaction," *Journal of Magnetism and Magnetic Materials*, p. 174158, 2026.

42. M. Abbasi, F. Valeh, and S. Mahdavifar, "Ground-state phase diagram, higher-winding topology, and lifshitz criticality in an anisotropic four-spin xx chain," *arXiv preprint arXiv:2609.03766*, 2026.

43. M. Abbasi and S. Mahdavifar, "Fermi-point topology determines emergent conformal criticality in extended quantum spin chains," *arXiv preprint arXiv:2609.03708*, 2026.

44. N. Kurdadze, G. Gogaberishvili, and G. Japaridze, "Critical phases of the extended isotropic *xy* chain with four-spin interaction," *arXiv preprint arXiv:2607.29006*, 2026.

45. S. Kimura, H. Yashiro, K. Okunishi, M. Hagiwara, Z. He, K. Kindo, T. Taniyama, and M. Itoh, "Field-induced order-disorder transition in antiferromagnetic baco 2 v 2 o 8 driven by a softening of spinon excitation," *Physical review letters*, vol. 99, no. 8, p. 087602, 2007.

46. Y. Kawasaki, J. L. Gavilano, L. Keller, J. Schefer, N. B. Christensen, A. Amato, T. Ohno, Y. Kishimoto, Z. He, Y. Ueda, *et al.*, "Magnetic structure and spin dynamics of the quasi-one-dimensional spin-chain antiferromagnet baco 2 v 2 o 8," *Physical Review B—Condensed Matter and Materials Physics*, vol. 83, no. 6, p. 064421, 2011.

47. S. Trotzky, P. Cheinet, S. Folling, M. Feld, U. Schnorrberger, A. M. Rey, A. Polkovnikov, E. A. Demler, M. D. Lukin, and I. Bloch, "Time-resolved observation and control of superexchange interactions with ultracold atoms in optical lattices," *Science*, vol. 319, no. 5861, pp. 295–299, 2008.

48. Y.-A. Chen, S. Nascimbene, M. Aidelsburger, M. Atala, S. Trotzky, and I. Bloch, "Controlling correlated tunneling and superexchange interactions with ac-driven optical lattices," *Physical review letters*, vol. 107, no. 21, p. 210405, 2011.

49. P. N. Jepsen, W. W. Ho, J. Amato-Grill, I. Dimitrova, E. Demler, and W. Ketterle, "Transverse spin dynamics in the anisotropic heisenberg model realized with ultracold atoms," *Physical Review X*, vol. 11, no. 4, p. 041054, 2021.

50. H. Lin, "Exact diagonalization of quantum-spin models," *Physical Review B*, vol. 42, no. 10, p. 6561, 1990.

51. S. R. White, "Density-matrix algorithms for quantum renormalization groups," *Physical review b*, vol. 48, no. 14, p. 10345, 1993.

52. U. Schollwöck, "The density-matrix renormalization group," *Reviews of modern physics*, vol. 77, no. 1, pp. 259–315, 2005.

53. D. Dmitriev, V. Y. Krivnov, and A. Ovchinnikov, "Gap generation in the xxz model in a transverse magnetic field," *Physical Review B*, vol. 65, no. 17, p. 172409, 2002.

54. S. Mahdavifar, S. Mahdavifar, and R. Jafari, "Magnetic quantum correlations in the one-dimensional transverse-field xxz model," *Physical Review A*, vol. 96, no. 5, p. 052303, 2017.

55. A. Osterloh, L. Amico, G. Falci, and R. Fazio, "Scaling of entanglement close to a quantum phase transition," *Nature*, vol. 416, no. 6881, pp. 608–610, 2002.

56. L. Amico, R. Fazio, A. Osterloh, and V. Vedral, "Entanglement in many-body systems," *Reviews of modern physics*, vol. 80, no. 2, pp. 517–576, 2008.

57. R. Horodecki, P. Horodecki, M. Horodecki, and K. Horodecki, "Quantum entanglement," *Reviews of modern physics*, vol. 81, no. 2, pp. 865–942, 2009.

58. N. Laflorencie, "Quantum entanglement in condensed matter systems," *Physics Reports*, vol. 646, pp. 1–59, 2016.

59. A. Bera, T. Das, D. Sadhukhan, S. Singha Roy, A. Sen, and U. Sen, "Quantum discord and its allies: a review of recent progress," *Reports on Progress in Physics*, vol. 81, no. 2, p. 024001, 2018.

60. D. Braun, G. Adesso, F. Benatti, R. Floreanini, U. Marzolino, M. W. Mitchell, and S. Pirandola, "Quantum-enhanced measurements without entanglement," *Reviews of Modern Physics*, vol. 90, no. 3, p. 035006, 2018.

61. W. K. Wootters, "Entanglement of formation of an arbitrary state of two qubits," *Physical Review Letters*, vol. 80, no. 10, p. 2245, 1998.

62. H. Ollivier and W. H. Zurek, "Quantum discord: a measure of the quantumness of correlations," *Physical review letters*, vol. 88, no. 1, p. 017901, 2001.

63. T. J. Osborne and M. A. Nielsen, "Entanglement in a simple quantum phase transition," *Physical Review A*, vol. 66, no. 3, p. 032110, 2002.

64. G. Vidal, J. I. Latorre, E. Rico, and A. Kitaev, "Entanglement in quantum critical phenomena," *Physical review letters*, vol. 90, no. 22, p. 227902, 2003.

65. L.-A. Wu, M. S. Sarandy, and D. Lidar, "Quantum phase transitions and bipartite entanglement," *Physical review letters*, vol. 93, no. 25, p. 250404, 2004.

66. Ö. Legeza and J. Sólyom, "Two-site entropy and quantum phase transitions in low-dimensional models," *Physical review letters*, vol. 96, no. 11, p. 116401, 2006.

67. F. K. Fumani, S. Nemati, S. Mahdavifar, and A. H. Darooneh, "Magnetic entanglement in spin-1/2 xy chains," *Physica A: Statistical Mechanics and its Applications*, vol. 445, pp. 256–263, 2016.

68. M. Soltani, F. K. Fumani, and S. Mahdavifar, "Ising in a transverse field with added transverse dzyaloshinskii-moriya interaction," *Journal of Magnetism and Magnetic Materials*, vol. 476, pp. 580–588, 2019.

69. E. Mehran, S. Mahdavifar, and R. Jafari, "Publisher's note: Induced effects of the dzyaloshinskii-moriya interaction on the thermal entanglement in spin-1/2 heisenberg chains [phys. rev. a 89, 042306 (2014)]," *Physical Review A*, vol. 89, no. 4, p. 049903, 2014.

70. F. K. Fumani, B. Beradze, S. Nemati, S. Mahdavifar, and G. Japaridze, "Quantum correlations in the spin-1/2 heisenberg xxz chain with modulated dzyaloshinskii-moriya interaction," *Journal of Magnetism and Magnetic Materials*, vol. 518, p. 167411, 2021.

71. S. Satoori, S. Mahdavifar, and J. Vahedi, "Entanglement and quantum correlations in the xx spin-1/2 honeycomb lattice," *Scientific Reports*, vol. 12, no. 1, p. 17991, 2022.

72. J. Jahangiri, M. Abbasi, and S. Mahdavifar, "Quantum correlations in spin-1/2 xxz chains with modulated magnetic fields and modulated dzyaloshinskii–moriya interaction," *Chinese Journal of Physics*, vol. 83, pp. 73–85, 2023.

73. S. Satoori, S. Mahdavifar, and J. Vahedi, "Quantum correlations in the frustrated xy model on the honeycomb lattice," *Scientific reports*, vol. 13, no. 1, p. 16034, 2023.

74. N. Mahboob, S. Mahdavifar, and F. Khastehdel Fumani, "Ground state analysis of the spin-1/2 xx chain model with anisotropic three-spin interaction," *SciPost Physics Core*, vol. 8, no. 3, p. 050, 2025.

75. S. Katibzadah, S. Mahdavifar, B. Haghdoust, F. K. Fumani, and M. Soltani, "Quantum discord as a probe of topological transitions in the spin-1/2 xx chain with four-spin interaction: S. katibzadah et al.," *Quantum Information Processing*, vol. 25, no. 2, p. 51, 2026.